Check for updates

Role of mesoscale eddies in the biogeochemistry of the Mozambique Channel

Fanny Chenillat[1]*, Eloise Deshaies[1], Aline Arens[1] and Pierrick Penven[2]*

[1]Actimar S.A.S., Brest, France, [2]Univ. Brest, CNRS, IRD, Ifremer, Laboratoire d'Océanographie Physique et Spatiale, IUEM, Brest, France

This study aims to characterize how eddies shape the biogeochemistry of the Mozambique Channel using a physical-biogeochemical model that realistically simulates its interannual dynamics. The 20-year-long numerical simulation provides a comprehensive dataset for robust statistical analysis of thousands of mesoscale features using an eddy detection method. We show that all eddy types significantly shape the biogeochemical landscape over the Mozambique Channel, with varying effects across different areas: (1) Sofala Bank and Delagoa Bay: Cyclonic eddies enhance diatom production. (2) Comoros Basin: Cyclonic eddies favor diatom growth via nutrient-rich waters from the NEMC. (3) Central Mozambique Channel: Anticyclonic eddies and rings promote nanophytoplankton through eddy-topography interactions. (4) Southern Mozambique Channel: A mix of eddies from the MC and South Madagascar influences diverse responses due to coastal upwelling. This diversity of processes results in distinct biological signatures of eddy types, leading to diverse ecosystem assemblages with a clear oligotrophic signature.

1 Introduction

The Mozambique Channel (MC) is of particular interest due to its dynamic nature, resulting from mesoscale activity that influences current dynamics and upwelling, with subsequent effects on biological productivity (Lutjeharms and Da Silva, 1988; Lutjeharms, 2006; Lamont et al., 2010). The MC is located in the Indian Ocean, along the eastern coast of Africa, extending from northern Madagascar to the southwestern tip of South Africa (Lutjeharms, 2006). It is part of the larger Agulhas Current System, which brings warm and salty waters into the Atlantic Ocean and plays a major role in the global meridional overturning of ocean circulation (de Ruijter et al., 1999) and climate change. The wind regime in the region is an extension of the northern Indian Ocean monsoon, where the

wind blows from the northeast during austral summer (prevailing from August to April) and from the southwest during austral winter (with maximum wind speed in June and July) (Sætre and Da Silva, 1979). The South Equatorial Current (SEC), which flows westward, divides into the Northeast Madagascar Current (NEMC) and the Southeast Madagascar Current (SEMC). The southward retroflection of the NEMC, forming the Mozambique Current, after being deflected by the coastline, triggers eddy formation near the Comoros islands, resulting in high turbulence in the narrow MC (Schouten et al., 2003). The MC is recognized as one of the most turbulent regions in the world, characterized by significant mesoscale activity (Chelton et al., 2007).

Eddies in the MC can be divided into two categories: eddies and rings. Cyclonic and anticyclonic eddies are generated through baroclinic instabilities at the scale of the Rossby radius of deformation. While anticyclonic eddies are mostly generated in the northern MC, cyclonic eddies are mainly generated along the eastern boundary of the MC by the formation of lee coastal-trapped cyclonic eddies (Lutjeharms, 2006). Cyclonic eddies propagate southwestward, while anticyclonic eddies move southward along the African coast (Halo et al., 2014a). Along the Mozambique shelf, dipoles of eddies often form, creating intense frontal zones (Marsac et al., 2014; Roberts et al., 2014). Significant eddy activity is also observed around the southern part of Madagascar (Halo et al., 2014b), where cyclonic eddies are generated by friction at the inshore edge of the southern extension of the Southeast Madagascar Current with the continental shelf. These eddies form as the current flows past the southern tip of Madagascar and migrates into the southern MC (Quartly et al., 2006; Morrow et al., 2004; Halo et al., 2014a). The MC is characterized by large anticyclonic eddies called rings (Halo et al., 2014a), which present different dynamical properties than eddies: larger diameter, deeper signature, higher vorticity, and longer duration than small anticyclonic eddies (Castelão and Johns, 2011; Halo et al., 2014a). Rings are generated through barotropic instability processes in the northern MC and propagate southward through the channel, along the African coast (Schouten et al., 2003; Halo et al., 2014a; Huang et al., 2024).

In terms of biogeochemistry, the MC is characterized by oligotrophic conditions, low surface chlorophyll-a, and a deep Chlorophyll-a maximum (DCM), which contributes significantly to the overall primary production of the water column (Lamont et al., 2014). On average, the most productive areas are the continental shelf Sofala Bank, Delagoa Bight, and Angoche regions, due to local and episodic upwelling driven by the interaction of mesoscale eddies with the continental slope (José et al., 2014; Lamont et al., 2014; Huggett and Kyewalyanga, 2017). Productivity in the Sofala Bank can also be influenced by the Zambezi Delta discharge (Leal et al., 2009). Coastal waters can be entrained at the eddy periphery by lateral advection (Williams and Follows, 1998) or be trapped in the eddy core (see Swart et al., 2010 for details), transporting enriched coastal waters offshore and driving cross-shelf fluxes of nutrients and biological material to the oligotrophic open ocean (Chenillat et al., 2016). Eddies and rings flowing southward along the African coast interact with the shelf, and the strong currents at their edge can entrain high coastal

biomass further offshore (Lamont et al., 2014). Eddies can also modulate local biological production through vertical local nutrient enrichment into the euphotic layer (McGillicuddy et al., 2007, 2016; Gaube et al., 2013, 2014, 2015; Chenillat et al., 2015). Such mesoscale eddies play a key role from the planktonic ecosystems up to the highest trophic levels: the frontal zone at the edges of eddies represents preferred foraging spots for top predators such as great frigatebirds contrasting to tunas that feed both in the cores and in the frontal zones of the eddies (Weimerskirch et al., 2004; Tew-Kai and Marsac, 2009; Della Penna and Gaube, 2020; Arostegui et al., 2022).

It is important to emphasize that mesoscale physical-biological-biogeochemical interactions can vary regionally (Gaube et al., 2014; Guo et al., 2019; Harrison et al., 2018), but on average, mesoscale eddies can enhance up to 30% of the total nitrate flux to the ocean surface euphotic layer (McGillicuddy et al., 2003), increasing primary production. While it is believed that anticyclonic eddies are nutrient-depleted with low rates of primary production and that cyclonic eddies are nutrient-enriched favoring high primary production (Tew-Kai and Marsac, 2009; Huggett and Kyewalyanga, 2017; Langa and Calil, 2020), there are contrasting results on the biogeochemical role of cyclonic/anticyclonic eddies with enhancing and suppressing effects depending on the location (José et al., 2016) and with various planktonic ecosystem assemblages (Ning et al., 2021). During their lifetime (formation, maturation, and decay), eddies can indeed shelter contrasting ecosystem assemblages (Chenillat et al., 2015; Schulien et al., 2020).

Here, we aim to elucidate how eddies shape the biogeochemistry of the MC by coupling a physical-biogeochemical model to realistically simulate the interannual dynamics of the MC. The 20-year numerical simulation provides a comprehensive dataset to perform a robust statistical analysis of thousands of mesoscale features using an eddy detection method. The methodology is described in section 2. In section 3, we explore the contrasting roles of cyclonic eddies, anticyclonic eddies, and rings. We present the average pattern of biogeochemical properties for each type of eddy, as well as their spatial signature throughout the region. We show that all eddy types of the Mozambique Channel, cyclonic eddies, anticyclonic eddies, and rings, have a positive influence on biogeochemistry on average. However, this positive biological signature differs from eddy types and leads to different ecosystem assemblages. In response to intense ocean dynamics, the biogeochemical signature in rings is exacerbated compared to smaller anticyclones.

2 Materials and methods

2.1 Ocean circulation and biogeochemical model

The Coastal and Regional Ocean Community (CROCO) model is an evolution of the three-dimensional ocean ROMS model that uses the Boussinesq approximation and hydrostatic vertical momentum balance to resolve the primitive equations on a rotating frame (Shchepetkin and McWilliams, 2005).

The SouthWest indiAn subtropical Gyre (SWAG12) grid configuration spans a geographical area from 6.8°W to 68.0°E, and from 47.5°S to 6.0°S, with a horizontal resolution of 1/12° and 75 terrain-following vertical levels on new Sigma coordinates (thetaS=5; thetaB=2; Hc=100). Surface forcings are provided by a bulk formulation using the daily ERA-5 atmospheric reanalysis (with a resolution of 1/4°; Hersbach et al., 2020) with a relative wind approach (Renault et al., 2017). PISCES is a biogeochemical module that has been implemented into CROCO with plankton compartments represented by two phytoplankton types (nanophytoplankton and diatoms) and two zooplankton types (microzooplankton and mesozooplankton) [see details in Aumont et al. (2015)].

Monthly outputs from the 1/4° GLORYS2v4 ocean reanalysis were used to force the boundaries of SWAG122 from 1993 to 2016. GLORYS2v4 is the non-assimilated version of GLORYS, including biogeochemical variables from the PISCES model. The initial condition in January of 1993 was also obtained from the 1/4° GLORYS2v4 ocean reanalysis. A simulation was conducted for 27 years (1991-2017), which included a spin-up of seven years (1991-1997). Three-day averages of model parameters are recorded to calculate eddy statistics in the MC.

This coupled model shows good agreement with physical and biogeochemical observations (see Supplementary Material, Supplementary Figures S1-S7). In particular, the eddy kinetic energy is well represented with high values in the eastern part of the channel, along the African coast (Supplementary Figure S1), which is characteristic of the rings distribution (Halo et al., 2014a). The cross-shore gradient of surface chlorophyll-a (Chl-a) is well captured with higher concentration found over the shelf, consistent with satellite observations (Supplementary Figure S5). The maximum Chlorophyll-a concentration is found in the subsurface, representing the DCM, and is largely dominated by nanophytoplankton as observed by Barlow et al. (2014) (Supplementary Figure S8). The south-to-north gradient of physical and biogeochemical properties along 41°E is also consistent with observations (Supplementary Figures S6-S8). The seasonal evolution of chlorophyll-a (Supplementary Figures S9, S13) is coherent with literature, with a bloom of nanophytoplankton peaking in August (Lévy et al., 2007; Tew-Kai and Marsac, 2009). This winter boreal bloom is concomitant with higher nutrient concentrations, especially nitrate and phosphate (Supplementary Figures S9, S11). Note that river inputs are not considered in the coupled model; Thus, the increase in nutrients over the shelf and the southern MC (Supplementary Figures S11, S12) is likely due to wind-driven cool-water upwelling (Lamont et al., 2014; Malauene et al., 2014) and the deepening of the mixed layer depth (MLD) induced by seasonal wind intensification and negative surface heat flux (Chiswell et al., 2015). Furthermore, there is a strong contrast with the open ocean over the Sofala Bank and Delagoa Bight with low SST and high SSS (Supplementary Figure S10), typical of upwelling conditions driven by eddy interaction with the shelf, thereby enhancing productivity (José et al., 2014; Lamont et al., 2014; Huggett and Kyewalyanga, 2017). Indeed, the Sofala Bank is one of the most productive regions off the Mozambican coast (Sá et al., 2013), as reproduced by the model (Supplementary Figures S13, S14). Diatom concentrations are,

on average, very weak and are confined to the Sofala Bank and Delagoa Bight during the boreal spring and summer, with Chl-a concentrations representing about 1/3 of the total Chl-a (Supplementary Figure S13). Over the Mascarene Basin, the model represents a weak increase in diatoms and nutrient concentrations (nitrate and phosphate, more pronounced in boreal winter, Supplementary Figures S9–S12), coherent with the upwelling of nutrient-rich waters, which increases chlorophyll concentration and secondary production levels downstream (Gallienne and Smythe-Wright, 2005). Consequently, the intrusion of the SEC and the NEMC into the MC is likely to transport different water masses - in terms of biogeochemical composition - depending on the seasonal cycle (Schouten et al., 2003) and to increase the amplitude of the seasonal variation of chlorophyll-a in the Mozambique Channel (Omta et al., 2009).

2.2 Eddy detection method and eddy tracking

To quantify the average properties of mesoscale eddies, we detect eddies in the 20-year run using the py-eddy-tracker method (Mason et al., 2014), an open-access tool based on the method of Chelton et al. (2011), which seeks the outermost closed contours of the SSH. Closed contours of the SSH are identified at 2 cm intervals. Non-eddy features are filtered by applying a battery of tests (e.g., shape test, size test, SSH extreme value test – see Supplementary Material, section 4 and Supplementary Figure S15, for details). The py-eddy tracker has been successfully used to study the eddy properties from numerical simulations (Mason et al., 2017, 2019; Smith and Fortin, 2022) and is used by CMEMS on satellite observations (Mason et al., 2019). This method is robust and exhibits low sensitivity to the parameters involved in the closed contour tests. The eddy detection was performed over the MC, [30-50°E; 10-30°S] on the 20 years of simulation (1998-2017): for every single eddy, its position, radius, and amplitude are recorded. From the eddy detection method, the radius is estimated according to their maximum speed (speed radius) or the closed contour area (effective radius). In this study, we focus our analysis on the speed criteria that presumably delimit the eddy core, i.e., the solid body rotation of the eddy.

Eddies were tracked by comparing the eddy center position at consecutive time steps over the entire run. Cyclone and anticyclone tracks are treated separately. The distances between all identified positions between two-time steps are calculated using the ellipse method of Chelton et al. (2011). If multiple vortices fall within the ellipse, in this case, the vortex is assigned according to the minimum of a set of dimensionless similarity parameters, S (Penven et al., 2005), computed for each t+1 candidate, as follows:

$$S_{t,t+1} = \sqrt{\left(\frac{\Delta d}{d_0}\right)^2 + \left(\frac{\Delta a}{a_0}\right)^2 + \left(\frac{\Delta A}{A_0}\right)^2},$$

Where Δd is the eddy separation distance at times t and $t+1$, Δa is the eddy area variation (based on L_{spd}), and ΔA is the amplitude variation. Characteristic values for eddy separation distance, area, and amplitude are given by d_0, a_0, and A_0, where $d_0 = 25km$, $a_0 = \pi 60^2 km^2$, and $A_0 = 2cm$, respectively. From the eddy

trajectories, the eddy lifetime can be estimated. We select long-lived eddies for trajectories longer than 30 days (Chelton et al., 2011; Halo et al., 2014a). From there, the velocity, direction of propagation, and evolution of biogeochemical properties along eddy trajectories can be evaluated.

The eddy detection and tracking analyses were also applied to the AVISO dataset, and the eddy characteristics from the model and the observation are in good agreement (Supplementary Figures S16-S19). According to the good agreement of both the water properties and the mesoscale activity characteristics, we are confident with the statistical analysis described below.

2.3 Eddy composite: an average eddy analysis approach

To assess the vertical and radial structure of the primary eddy characteristics, a composite analysis was conducted regardless of the eddy lifetime. The composite analysis consisted of computing an average eddy over all detected eddies. The computed normalized radius R corresponds to the boundary of the eddy core, the speed radius. To account for the region surrounding the eddy core, the composite is performed over 3R. The R-normalized horizontal coordinates were used for each eddy, and the physical and biogeochemical properties were averaged across all eddies in this normalized coordinate system, where the eddy center was at 0 and the eddy core's edge was at ±1R. The eddy core is limited to ±1R (the solid body rotation area); The region surrounding the eddy is assumed to be far from the eddy core limit and we arbitrarily choose ±2R as a minimum limit; Between the eddy core limit and the surrounding eddy limit, the region is defined as the edge of the eddy.

To spatially evaluate the local influence of eddies, we calculate Individual eddy property anomalies, by computing the difference between the eddy core ($R \in [-1; +1]$) and the area surrounding the outermost eddy limit ($R \geq |(2.7)|$), averaged over 100m depth. The area surrounding can be linked to the non-eddy structure. An eddy anomaly indicates the relative local impact of eddies.

Finally, the north-to-south vertical impact of eddies was diagnosed and compared to the 20-year climatology to better appreciate the spatial impact of eddies according to latitudinal and vertical gradients.

3 Results and discussion: mesoscale modulation of biogeochemistry

3.1 Mesoscale properties in the Mozambique Channel

Over the 20-year simulation, we identified 19561 cyclonic eddies and 14769 anticyclonic eddies over the MC (from 13.5°S to 25°S), i.e., 978 cyclonic and 738 anticyclonic observations per year. One-third of identified anticyclonic eddies are rings [using the radius criteria ≥ 100km, as in Halo et al. (2014a)], with a total of 4400 entities detected. Mean radius and speed are 60km and 6.4km/day

for cyclonic eddies, 58km and 6.5km/day for anticyclonic eddies (with R<100km), and 127km and 10.5km/day for rings, consistently with prior observations (Halo et al., 2014a; Schouten et al., 2003).

Cyclonic and anticyclonic eddies are heterogeneously distributed in the MC (Figures 1A, B) in agreement with the surface eddy kinetic energy map (Supplementary Material). Cyclonic eddies are fairly ubiquitous in the channel, but long-lived ones are mainly found in the eastern part of the channel, in agreement with Halo et al. (2014a). Another site of high concentration for long-lasting cyclonic eddies is located in the northwestern region of Madagascar, at the northern entrance of the channel, as mentioned by Halo et al. (2014a). Cyclonic eddies are slightly more abundant during the first half of the year (Figure 1C). We tracked 571 trajectories of cyclonic long-lived eddies, with various patterns: cyclonic eddies along the African coast traveled southward with an offshore component. In contrast, northern cyclonic eddies traveled westward with a small southward component. Cyclonic eddies forming in the eastern part of the channel from 15°S to 22.5°S traveled southwestward (Halo et al., 2014a). Cyclonic eddies can also form over the biologically productive African shelf (Leal et al., 2009; Paula et al., 1998), in Sofala Bank (Malauene et al., 2018), and more predominantly in the Delagoa Bight (Cossa et al., 2016). Anticyclonic eddies are distributed throughout the channel, except over the African shelf of Sofala Bank where the formation of short-lived cyclonic eddies dominates. Notably, persistent anticyclonic eddies, such as rings, are concentrated within the 'eddy corridor' along the Mozambique shelf edge. This phenomenon follows the underlying topography, spanning approximately 100 to 500 kilometers offshore. These anticyclonic eddies travel southward toward the Agulhas system, as documented by Malauene et al. (2018); Schouten et al. (2003); Quartly et al. (2013), and Halo et al. (2014a).

We found 455 and 278 tracks of long-lived anticyclonic eddies and rings, i.e., 23 and 14 tracks per year, respectively. Restricted to a region spanning 1/2° around 17°S we found ~5 ring tracks per year, consistent with the literature (de Ruijter et al., 2002; Halo et al., 2014a; Schouten et al., 2003). Most anticyclonic eddies and rings occur in the first quarter of the year (39% in January-February-March).

3.2 Effect of mesoscale activity on the planktonic ecosystem

While the most limiting nutrients in the western Indian Ocean are generally nitrate and phosphate, with silicate being more accessible (Barlow et al., 2007; Kyewalyanga et al., 2007; Leal et al., 2009; Sá et al., 2013), nitrate is recognized as the primary factor limiting phytoplankton production in the MC (Koné et al., 2009). Therefore, our study focuses only on nitrate and Chl-a in nanophytoplankton and diatoms. All analyses related to the other nutrients and zooplankton are provided in the Supplementary Material (Supplementary Figure S20).

Figure 2 illustrates the distinct cross-shore properties of cyclonic eddies, anticyclonic eddies, and rings. Cyclonic eddies
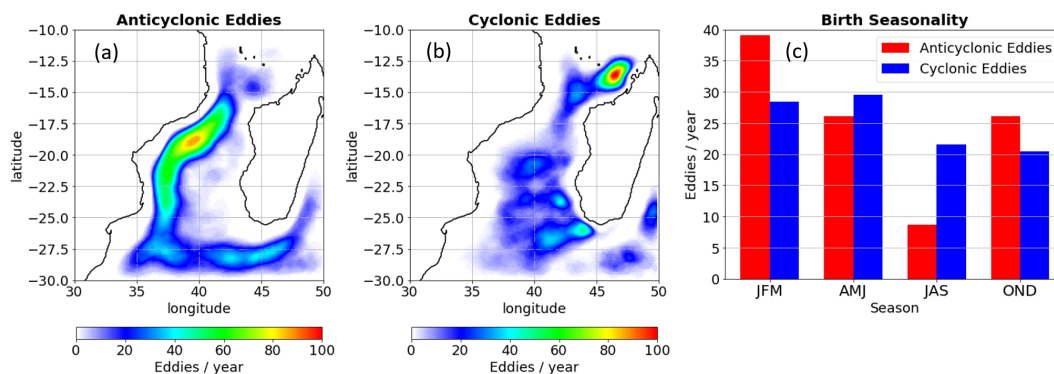
FIGURE 1
Distribution of eddies per year for **(A)** anticyclonic eddies and **(B)** cyclonic eddies, and **(C)** seasonality of long-lived (>30 days) eddies located in the MC (from 13.5°S to 25°S). Eddy distribution represents the area covered by the eddy core as defined in Materials and Methods. JFM, AMJ, JAS, and OND refer to seasonal averages of January-February-March, April-May-June, July-August-September, and October-November-December, respectively.

display an upward doming signature of isotherms, isohalines, and isolines of nitrate, all reaching about 25m. Symmetrically, anticyclonic eddies exhibit a downward bend of about 25 meters, characterized by warm and fresh waters, slightly depleted in nitrate in the core. The downwelling in rings is even more pronounced with isolines deepening to ~50m with overexpressed gradients. It is important to note that the surrounding (for R> ± 2) physical and biogeochemical properties of cyclonic eddies, anticyclonic eddies, and rings exhibit differences. This disparity is mostly due to the spatial distribution of each eddy type associated with large-scale water masses gradients (see Supplementary Figures S3, S5, S10). Note also that the vertical profile of salinity for all composites is typical of the region (Supplementary Figure S4) with a vertical inverse gradient: saltier waters are at the surface contrasting with fresher waters at depth.

Regarding the effect on phytoplankton, nitrate doming in the core of cyclonic eddies leads to a doubling of Chl-a in diatoms at 75m depth and a slight decrease in Chl-a in nanophytoplankton, compared to the surrounding areas. Such a shift in the ecosystem assemblage (an increase in diatoms and a decrease in nanophytoplankton) is likely driven by vertical nutrient input from eddy-pumping which favors diatom growth. There is also a slight surface signature of diatoms driven by the vertical mixing of the top of the DCM within the MLD. In anticyclonic eddies, the core shows a decrease in diatom Chl-a and no significant effect on nanophytoplankton Chl-a compared to the surrounding areas, however at the edge of the eddy there is a slight increase within the MLD (between ±1R and ±2R). This phenomenon is even more pronounced in the rings, where nitrate concentrations is higher in the surrounding areas especially at the eastern edge; this is associated with local increase of Chl-a in nanophytoplankton from the subsurface to the surface. Chl-a in diatoms is higher at the eastern edge of the rings due to the distribution of eddies near the African coast, where the eddy-topography interactions lead to strong nutrient enrichment (Marsac et al., 2014).

As expected, on average, cyclonic eddies positively influence primary production, likely through vertical advection of nutrients at

the base of the euphotic layer, in the subsurface at the DCM (Chenillat et al., 2016). In the DCM of cyclonic eddies, a stronger signature over diatoms occurs, which is note the case over nanophytoplankton. This highlights the role of cyclonic eddies in modifying planktonic community composition compared to the non-eddy environment (Pereira et al., 2024). On average, anticyclonic eddies slightly promote nanophytoplankton primary production at the edge, and rings drive a strong response of nanophytoplankton from the edge to the core: enriched shelf water is entrained around these anticyclonic structures and can be transported along isopycnals downward to the core and below the MLD, without surface signature. Both anticyclonic eddies and rings appear to be unfavorable for diatom growth due to limited vertical advection of nutrients. This statistical confirmation highlights the significance of eddy-topography interactions in influencing the biological production in the MC, as described by José et al. (2014), especially for rings. Cyclonic eddies could also be affected by eddy-topography interactions in terms of nutrient enrichment and primary production, but the main dynamics that is highlighted by this statistical analysis is the local vertical input from eddy-pumping. It should be noted that an additional impact of nutrient input from rivers is to be expected. However, this has not been considered in the context of the numerical experiment, and thus falls outside the scope of this study.

To better describe and disentangle the effect of eddies on biogeochemical properties, our analysis focuses on their regional influence. To do this, for each long-lived eddy, we compute the concentration anomalies of nitrate, Chl-a in nanophytoplankton, and Chl-a in diatoms between the eddy core and eddy surroundings, averaged over 0-100 m depth, reduced to the surrounding values to obtain a percentage (Figure 3).

Over the Sofala Bank and the Delagoa Bight, a significant increase in the concentration of chlorophyll-a and nitrate (and all other nutrients, Supplementary Figure S21) is observed in the cyclonic eddy cores when compared to the surrounding eddy regions. This finding is consistent with Lamont et al. (2014), which suggests that eddy-topography interactions play a role in
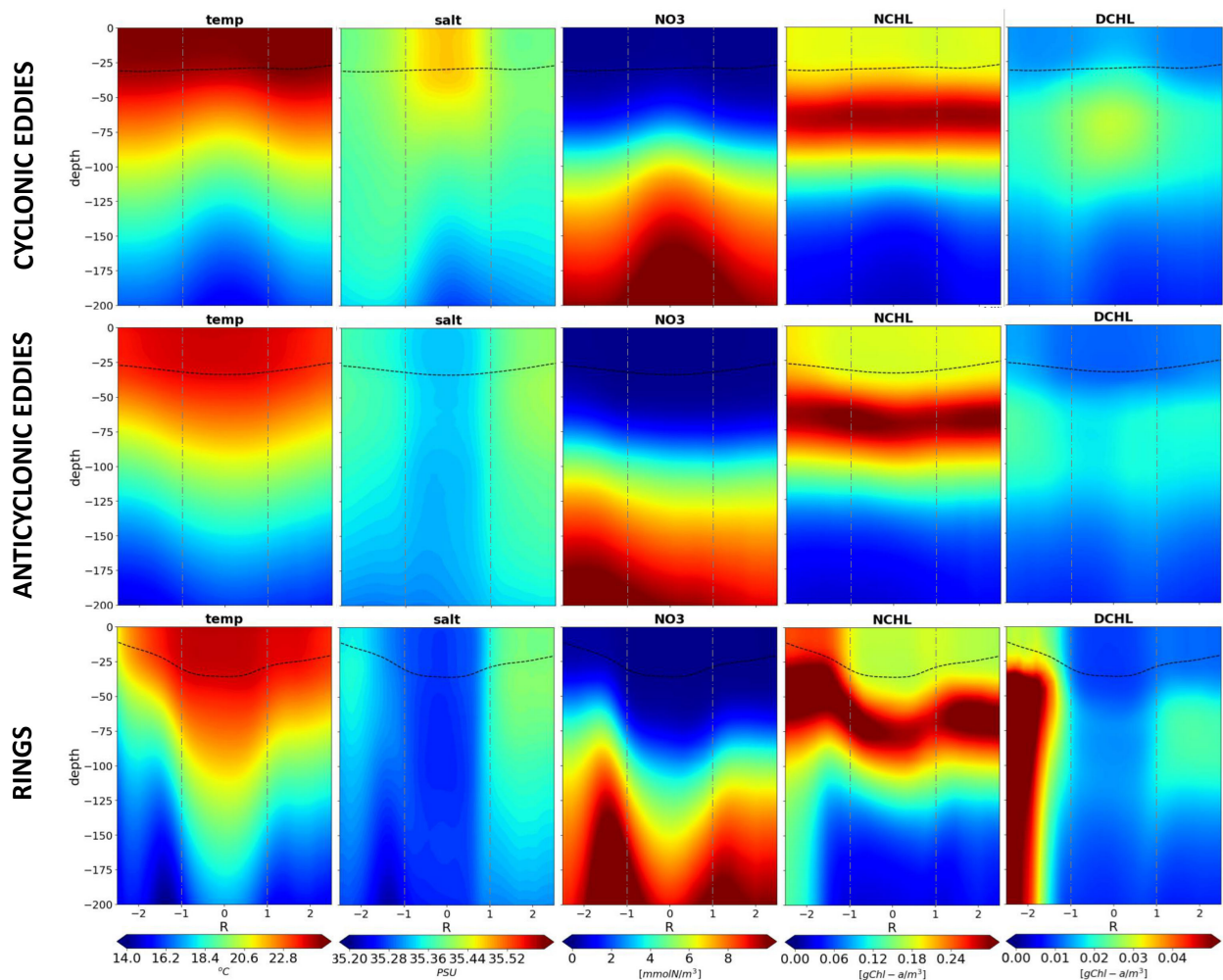
FIGURE 2
Average properties of (top row) cyclonic eddies, (middle row) anticyclonic eddies - without rings - and (bottom row) rings for eddies between 13.5°S and 20°S. From left to right: temperature, salinity, nitrate, Chl-a in nanophytoplankton, and Chl-a in diatoms. The composites represent the average profiles across eddies, with the eddy core centered at 0 and R the radius of the eddy core (positive R represents the eastern side). The dashed line represents the mixed layer depth. Vertical dashed grey lines indicate the eddy core limit ($\pm$ 1R).

the upwelling of deep, nutrient-rich waters favoring primary production (Leal et al., 2009). A Similar positive trend is observed over the central portion of the MC, from 15°S to 22.5°S, in open ocean waters, distant from potential eddy-topography interactions. It is noteworthy that this increase in the northern MC and over the shelf is considerably more pronounced for diatoms than for nanophytoplankton, indicating a potential shift in ecosystem composition compared to non-eddy areas, as suggested earlier. Such planktonic modulation can be explained by eddy pumping, whereby deeper, nutrient-rich waters are brought upward into the euphotic zone, favoring larger diatoms-like phytoplankton (Landry et al., 2008; Chenillat et al., 2016; Pereira et al., 2024). It is established that diatoms exhibit a rapid response to nutrient injections in the euphotic zone (Brown et al., 2008).

In the Comoros basin, cyclonic eddies cores also demonstrate positive trends of nitrate and Chl-a in diatoms (also observed for phosphate, silicate, and iron, and not consistently for Chl-a in nanophytoplankton, zooplankton, and ammonium, Supplementary

Figure S21). This is likely the result of the intrusion of significant quantities of upwelled nutrient-rich water from the NEMC, which interacts with eddies forming around Comoros (see Figure 1; Huang et al., 2024).

At the southern tip of Madagascar, the cores of cyclonic eddies present positive trends in nitrate and Chl-a. This region is known for its coastal upwelling (Machu et al., 2002) where cyclonic eddies trap and efficiently transport enriched upwelled water and associated ecosystem (Chenillat et al., 2016) to the southwest.

In the offshore region of the central MC, and mostly along the shelf, anticyclonic structures present a pronounced negative trend, which is consistent with low primary production in their core (Tew-Kai and Marsac, 2009). However, some positive trends can be observed confined along the entire shelf limit, which is particularly relevant for rings. These local positive trends concern mainly nitrate and Chl-a, mostly for nanophytoplankton (and all nutrients except silicate) off Angoche, south of Sofala bank, and in the southern region, at the onset of the Agulhas Current. Such
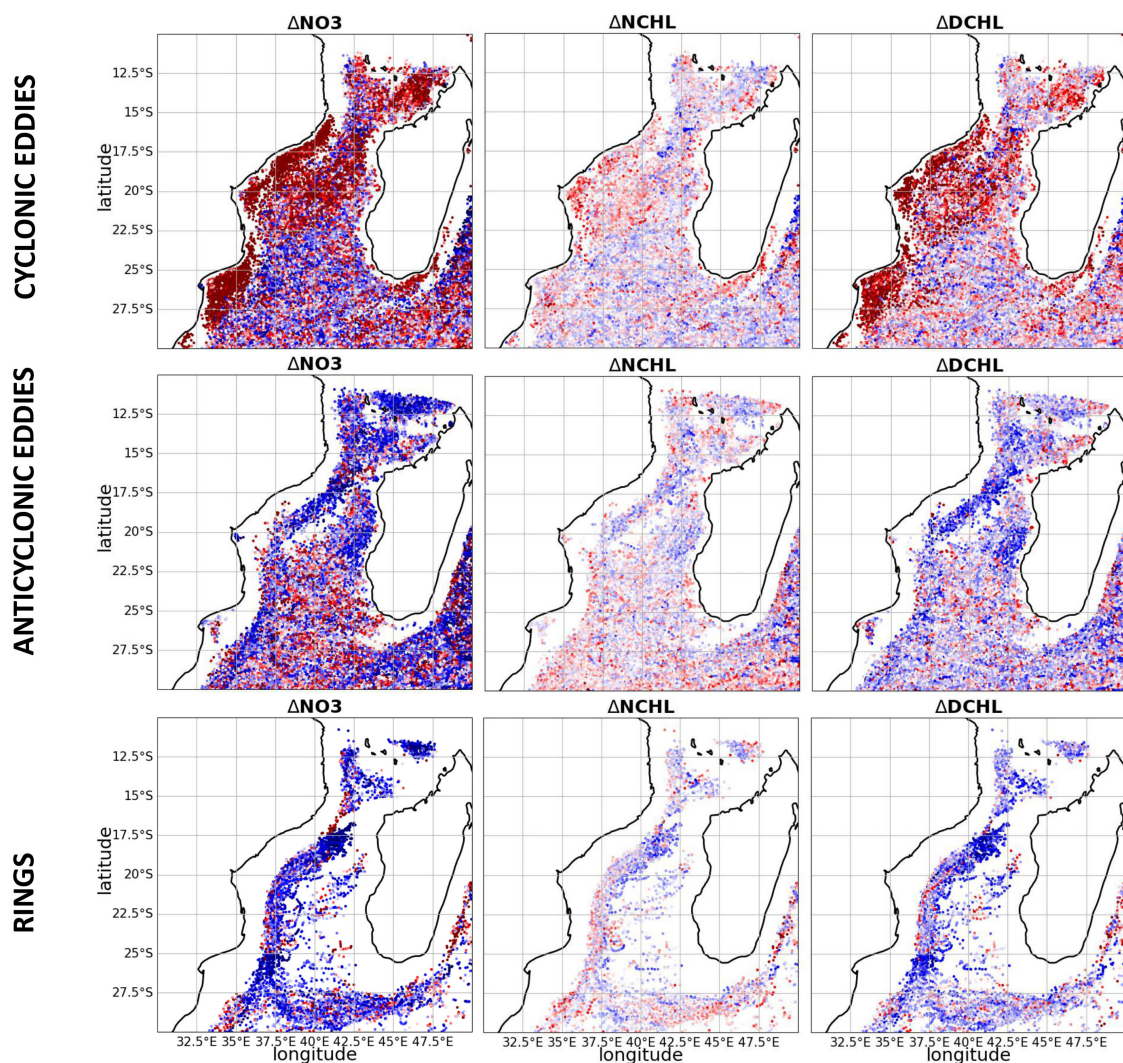
FIGURE 3

Anomalies between the eddy core and the area surrounding the eddy, averaged over 100m depth, expressed in percentage, in (top row) cyclonic eddies, (middle row) anticyclonic eddies, and (bottom row) rings, for nitrate (NO3), Chl-a in nanophytoplankton and Chl-a in diatoms.

enrichment in anticyclonic eddies has already been observed (Rodriguez et al., 2003; Waite et al., 2007), particularly in those interacting with the shelf, with material entrainment at their edges (Crawford et al., 2005; Moore et al., 2007). This highlights the suppressor effect of anticyclonic eddies on diatoms: anticyclonic eddies promote the trapping of coastal waters without substantial enrichment from deep water, thereby enabling the ecosystem to self-maintain through regenerated primary production. This limits the growth of diatoms-like phytoplankton and favors production by nanophytoplankton (Chenillat et al., 2015).

In the southern MC, a mixture of positive and negative signals is observed, with a majority of negative trends for cyclonic eddies and positive trends for anticyclonic eddies for all considered biogeochemical variables. This highlights more complex dynamics with several distinct processes at play. These include Ekman pumping in cyclonic eddies, lateral transport of material within eddies, and eddy-eddy interactions that interplay with the seasonal

fluctuations of different key processes, such as variability of the MLD, the euphotic depth, wind patterns, and biological dynamics.

In addition, we observed a significant latitudinal gradient in the water mass properties of the eddy cores along the MC (Figure 4 and Supplementary Figure S21). The climatology shows a southward increase in nutrients and Chl-a (Sá et al., 2013), along with a decrease in temperature and an increase in salinity, which induces a deepening of the DCM. A comparison between the north-to-south climatology and the eddies reveals a significant effect of eddies on the vertical redistribution of oceanic variables, characterized by shallower nutriclines and DCM, particularly in the region north of 25°S, strictly in the MC. The isolines of temperature, nutrients, the DCM, and the MLD are observed to be shallower in the north-to-south cyclonic eddies than in anticyclonic eddies and rings. This finding is consistent with the results presented in Figure 2. In comparison to the overall north-to-south average, the concentration of chlorophyll-a is higher within the cores of

cyclonic eddies than within anticyclonic eddies throughout the entire MC. The DCM of nanophytoplankton is present throughout the MC for all eddies and rings. In contrast, the DCM of diatoms is deeper and exhibits two distinct hotspots: one around 15°S and the other around 20°S, corresponding to the Angoche and the middle of Sofala Bank, respectively. These hotspots are also visible in anticyclonic eddies but are more pronounced in cyclonic eddies. The northern hotspot is also evident in the concentration of Chl-a in nanophytoplankton within cyclonic eddies. This phenomenon can be attributed to the high eddy generation occurring in northern Madagascar (Figures 1, 3) (José et al., 2016) combining the effect of strong nutrient vertical input in eddies favoring diatoms in deeper waters contrasting with lateral advection and trapping of coastal water as they move southward along the slope. This enrichment could be further enhanced by eddy/eddy interactions and offshore export of coastal water masses by filaments. These findings are consistent with previous studies (e.g., José et al., 2014; Roberts et al., 2014) and recent *in situ* observations of a filament situated between a dipole formed by a cyclonic eddy and a ring during the RESILIENCE cruise (doi:10.17600/18001917). From the northernmost point to 26°S, the DCM of nanophytoplankton remains high for all eddy types, compared to the climatology. This can be attributed to the retention of water masses and ability of eddies to support a phytoplanktonic production based on remineralization, below the MLD (Chenillat et al., 2015) as they move southward in the MC. With regards to the southern hotspot, elevated subsurface Chl-a concentrations around 20°S and 26°S are attributable to the coastal increase of plankton biomass over the shelf. Our findings indicate that anticyclonic eddies and rings exert limited control over diatom production. This may be due to the physical, biogeochemical, and ecological characteristics of the background water masses trapped by these entities, favoring regenerated production by nanophytoplankton.

4 Summary and conclusions

Biogeochemical properties in eddies of the MC were studied using a coupled physical-biological model that accurately reproduces the peculiar rich eddy mesoscale activity of the region and the main biological properties.

Applying the open-source py-eddy-tracker eddy-detection and eddy-tracking algorithm to the 20-year-long numerical simulation allowed us to quantify biogeochemical tracers within individual eddies: 19,561 cyclonic eddies, and 14,769 anticyclonic eddies and rings, occurring mostly in the first quarter of the year.

In cyclonic eddies, we found a strong positive biological signature associated with the doming of isolines within the core, likely to locally upwell deep nutrients to the subsurface, enhancing the subsurface production of diatoms, while nanophytoplankton still dominates the phytoplankton assemblage; this might be due to the background phytoplankton assemblage of surrounding waters that can be trapped by cyclonic eddies or also by the secondary production that can take place based on remineralization, at subsurface. In anticyclonic eddies, and more importantly in rings, we found a strong positive signature on nanophytoplankton and a very limited impact in diatoms; this can

be inferred from the ability of anticyclonic eddies to trap and retain surrounding waters and associated planktonic ecosystems that can evolve – likely based on remineralization - in the eddy core while the eddy is traveling. Indeed, for all eddy types, the subsurface maximum is largely dominated by nanophytoplankton, in higher proportion than in the background waters, from north to south. This is an indication of the retention of water in eddy cores, where an ecosystem can be maintained.

We emphasize the regional influence of eddies in driving or limiting nutrient enrichment and modulating primary production and planktonic ecosystem composition. Cyclonic eddies, which are ubiquitous across the MC, interact with nutrient-rich waters, promoting primary production in key areas. In contrast, anticyclonic eddies, particularly rings, are predominantly located in the western MC, where they induce significant nutrient enrichment through eddy-topography interactions. The mechanisms driving nutrient enrichment and enhanced primary production within eddies vary across regions:

1. Sofala Bank and Delagoa Bay: Coastally trapped cyclonic eddies promote diatom production by trapping nutrient-rich waters.
2. Comoros Basin: Cyclonic eddies interact with nutrient-rich waters from the NEMC, also favoring diatom growth.
3. Central Mozambique Channel: Anticyclonic eddies and rings dominate, with strong eddy-topography interactions that primarily support nanophytoplankton production.
4. Southern Mozambique Channel: A convergence of eddies from the MC and South Madagascar transports coastal upwelled waters, resulting in a complex array of responses.

To our knowledge, this is the first statistical analysis performed to describe the average role of eddies on nitrate and phytoplankton. Our findings corroborate the vital role of mesoscale features in the MC to feed higher trophic levels and shape the MC ecosystem in agreement with José et al. (2016), with various regional signature depending on eddy characteristics. We are aware that our approach does not consider the complexity of ecological response to specific eddy characteristics that could play a crucial biological role as the eddy origin (José et al., 2014) or eddy seasonality. Nevertheless, the statistical approach provides robust results regarding the average composition of eddies. Moreover, our coupled CROCO-PISCES configuration, which display coherent physical and biogeochemical dynamics, could be further explored in terms of biophysical interactions or biogeochemical processes, but also in terms of long-term variability, as the model has run for a 20-year inter-annual simulation. Further investigation is required to ascertain the relative contributions of lateral stirring and vertical pumping in the role of eddies concerning plankton production within eddies and rings. This should include quantification of the physical advection of nutrients and biological fluxes (new vs. regenerated production). Moreover, the incorporating of key processes, such as accounting for submesoscale features (by increasing model resolution), introducing tides, and coupling for ocean-atmosphere interactions could help modulate mesoscale activity. Indeed, submesoscale processes in frontal zones at the edge of eddies (Swart et al., 2010) and eddy dipoles (Lamont
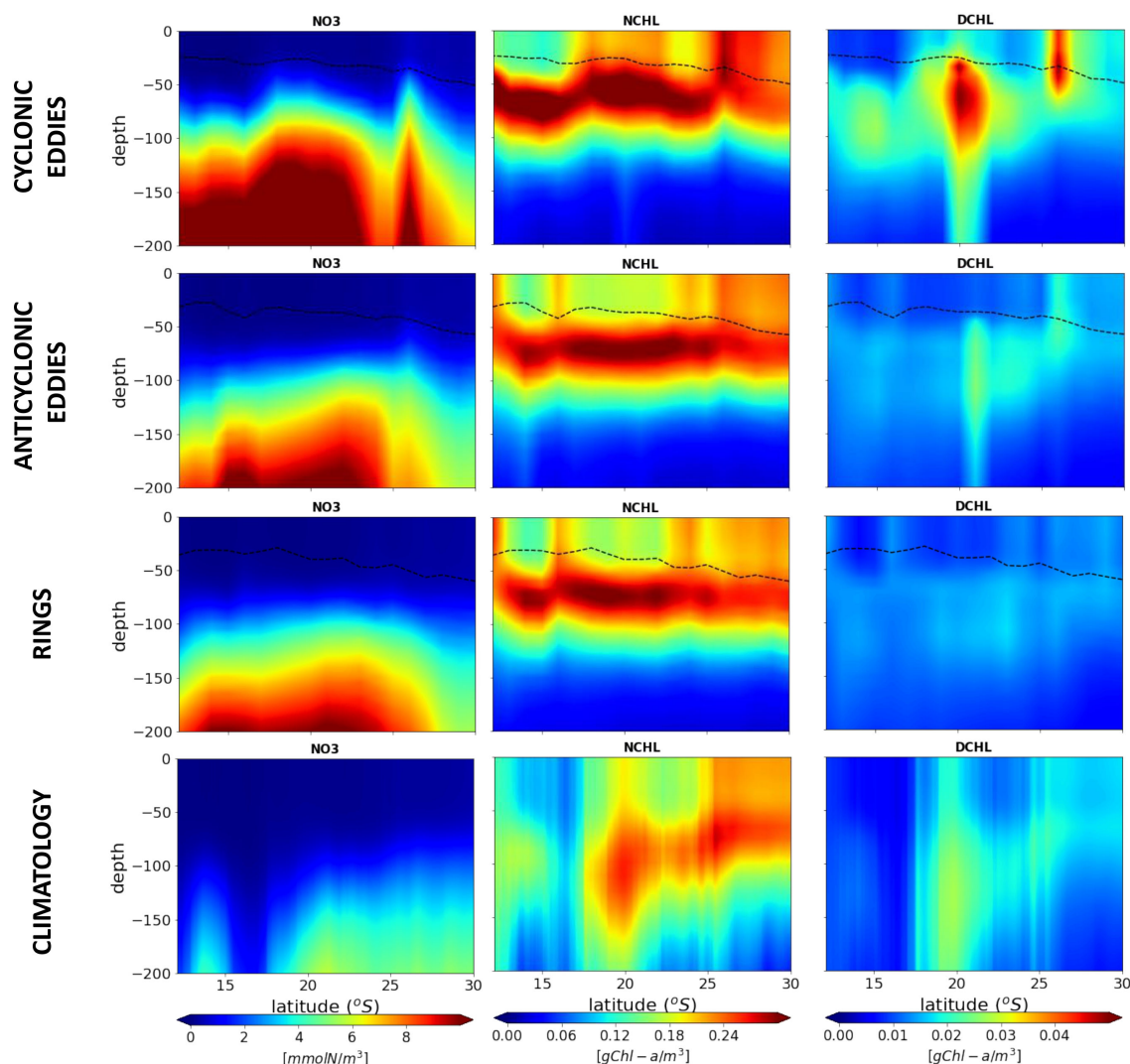
FIGURE 4
Latitudinal vertical sections of properties in (top row) cyclonic eddy cores, (second row) anticyclonic eddy cores (third row) rings core and (fourth raw) for 20-year climatology, averaged across the channel, for nitrate, Chl-a in nanophytoplankton and Chl-a in diatoms. The dashed line represents the mixed layer depth.

et al., 2014) have been demonstrated to produce cross-isopycnal fluxes, which drive local chlorophyll maximums (Pereira et al., 2024). Furthermore, it is imperative to consider the biogeochemical aspects of the system, including nutrient inputs from rivers, to gain a comprehensive understanding of eddy-driven plankton production. Finally, dedicated field campaigns are required to study the physical-biological processes of mesoscale and submesoscale features, and support and validate model results.

Data availability statement

The original contributions presented in the study are included in the article/Supplementary Material. Further inquiries can be directed to the corresponding authors. Model data are available on request. The identification and automated tracking of oceanic eddies tool here used is *py-eddy-tracker*, a free software tool available on GitHub. It is fully documented here https://py-eddy-tracker.readthedocs.io/en/stable/index.html.

Author contributions

FC: Conceptualization, Formal analysis, Investigation, Methodology, Supervision, Validation, Visualization, Writing – original draft, Writing – review & editing. ED: Formal analysis, Investigation, Visualization, Writing – review & editing. AA: Formal analysis, Investigation, Visualization, Writing – review & editing. PP: Conceptualization, Data curation, Funding acquisition, Methodology, Resources, Supervision, Validation, Writing – review & editing.

Conflict of interest

FC, ED and AA were employed by Actimar S.A.S.

The remaining author declares that the research was conducted in the absence of any commercial or financial relationships that could be construed as a potential conflict of interest.

Publisher's note

All claims expressed in this article are solely those of the authors and do not necessarily represent those of their affiliated organizations, or those of the publisher, the editors and the reviewers. Any product that may be evaluated in this article, or claim that may be made by its manufacturer, is not guaranteed or endorsed by the publisher.

Supplementary material

The Supplementary Material for this article can be found online at: https://www.frontiersin.org/articles/10.3389/fmars.2024.1402776/full#supplementary-material

References

Arostegui, M. C., Gaube, P., Woodworth-Jefcoats, P. A., Kobayashi, D. R., and Braun, C. D. (2022). Anticyclonic eddies aggregate pelagic predators in a subtropical gyre. *Nature* 609, 535–540. doi: 10.1038/s41586-022-05162-6

Aumont, O., Ethé, C., Tagliabue, A., Bopp, L., and Gehlen, M. (2015). PISCES-v2: an ocean biogeochemical model for carbon and ecosystem studies Geosci. *Model. Dev.* 8, 2465–2513. doi: 10.5194/gmd-8-2465-2015

Barlow, R., Lamont, T., Morris, T., Sessions, H., and van den Berg, M. (2014). Adaptation of phytoplankton communities to mesoscale eddies in the Mozambique Channel. *Deep Sea Res. Part II: Topical Stud. Oceanography* 100, 106–118. doi: 10.1016/j.dsr2.2013.10.020. ISSN 0967-0645.

Barlow, R., Stuart, V., Lutz, V., Sessions, H., Sathyendranath, S., Platt, T., et al. (2007). Seasonal pigment patterns of surface phytoplankton in the subtropical southern hemisphere. *Deep Sea Res. Part I: Oceanographic Res. Papers* 54, 1687–1703. doi: 10.1016/j.dsr.2007.06.010

Brown, S., Landry, M., Selph, K., Jin Yang, E., Rii, Y., and Bidigare, R. (2008). Diatoms in the desert: plankton community response to a mesoscale eddy in the subtropical North Pacific. *Deep-Sea Res. II* 55, 1321–1333. doi: 10.1016/j.dsr2.2008.02.012

Castelão, G. P., and Johns, W. E. (2011). Sea surface structure of North Brazil Current rings derived from shipboard and moored acoustic doppler current profiler observations. *J. Geophys. Res.* 116, CO1010. doi: 10.1029/2010JC006575

Chelton, D. B., Schlax, M. G., and Samelson, R. M. (2011). Global observations of nonlinear mesoscale eddies. *Prog. Oceanogr.* 91, 167–216. doi: 10.1016/j.pocean.2011.01.002

Chelton, D. B., Schlax, M. G., Samelson, R. M., and de Szoeke, R. A. (2007). Global observations of large oceanic eddies. *Geophys. Res. Lett.* 34, 1–5. doi: 10.1029/2007GL030812

Chenillat, F., Franks, P. J. S., and Combes, V. (2016). Biogeochemical properties of eddies in the California Current System. *Geophys. Res. Lett.* 43, 5812–5820. doi: 10.1002/2016GL068945

Chenillat, F., Franks, P. J. S., Rivière, P., Capet, X., Grima, N., and Blanke, B. (2015). Plankton dynamics in a cyclonic eddy in the Southern California Current System. *J. Geophys. Res. Oceans* 120, 5566–5588. doi: 10.1002/2015JC010826

Chiswell, S. M., Calil, P. H., and Boyd, P. W. (2015). Spring blooms and annual cycles of phytoplankton: a unified perspective. *J. Plankton Res.* 37, 500–508. doi: 10.1093/plankt/fbv02111

Cossa, O., Pous, S., Penven, P., Capet, X., and Reason, C. J. C. (2016). Modelling cyclonic eddies in the Delagoa Bight region. *Continental Shelf Res.* 119, 14–29. doi: 10.1016/j.csr.2016.03.006

Crawford, W. R., Brickley, P. J., Peterson, T. D., and Thomas, A. C. (2005). Impact of Haida eddies on chlorophyll distribution in the eastern Gulf of Alaska. *Deep Sea Res II Top Stud Oceanogr* 52 (7-8), 975–990. doi: 10.1016/j.dsr2.2005.02.011

Della Penna, A., and Gaube, P. (2020). Mesoscale eddies structure mesopelagic communities. *Front. Mar. Sci.* 7. doi: 10.3389/fmars.2020.00454

deRuijter, W. P. M., Biastoch, A., Drijfhout, S. S., Lutjeharms, J. R. E., Matano, R. P., Pichevin, T., et al. (1999). Indian-Atlantic interocean exchange: Dynamics, estimation and impact. *J. Geophys. Res.* 104, 20885–20910. doi: 10.1029/1998JC900099

de Ruijter, W. P., Ridderinkhof, H., Lutjeharms, J. R., Schouten, M. W., and Veth, C. (2002). Observations of the flow in the mozambique channel. *Geophysical Res. Lett.* 29 (10), 140–141. doi: 10.1029/2001GL013714

Gallienne, C. P., and Smythe-Wright, D. (2005). Epipelagic mesozooplankton dynamics around the Mascarene Plateau and Basin, Southwestern Indian Ocean. *Philos. Trans. R. Soc. London A: Mathematical Phys. Eng. Sci.* 363, 191–202. doi: 10.1098/rsta.2004.1487

Gaube, P., Chelton, D. B., Samelson, R. M., Schlax, M. G., and O'Neill, L. W. (2015). Satellite observations of mesoscale eddy-induced Ekman pumping. *J. Phys. Oceanogr.* 45, 104–132. doi: 10.1175/jpo-d-14-0032.1

Gaube, P., Chelton, D. B., Strutton, P. G., and Behrenfeld, M. J. (2013). Satellite observations of chlorophyll, phytoplankton biomass, and Ekman pumping in nonlinear mesoscale eddies. *J. Geophysical Research: Oceans* 118, 6349–6370. doi: 10.1002/2013JC009027

Gaube, P., McGillicuddy, D. J. Jr., Chelton, D. B., Behrenfeld, M. J., and Strutton, P. G. (2014). Regional variations in the influence of mesoscale eddies on near-surface chlorophyll. *J. Geophysical Research: Oceans* 119, 8195–8220. doi: 10.1002/2014JC010111

Guo, M., Xiu, P., Chai, F., and Xue, H. (2019). Mesoscale and submesoscale contributions to high sea surface chlorophyll in subtropical gyres. *Geophysical Res. Lett.* 46, 13217–13226. doi: 10.1029/2019GL085278

Halo, I., Backeberg, B., Penven, P., Reason, C., Ansorge, I., and Ulgren, J. (2014a). Eddy properties in the Mozambique Channel: a comparison between satellite altimetry and ocean circulation models. *Deep Sea Res. Part II* 100, 119–135. doi: 10.1016/j.dsr2.2013.10.015

Halo, I., Penven, P., Backeberg, B., Ansorge, I., Shillington, F., and Roman, R. (2014b). Mesoscale eddy variability in the southern extension of the East Madagascar Current: Seasonal cycle, energy conversion terms, and eddy mean properties. *J. Geophys. Res. Oceans* 119, 7324–7356. doi: 10.1002/2014JC009820

Harrison, C. S., Long, M. C., Lovenduski, N. S., and Moore, J. K. (2018). Mesoscale effects on carbon export: A global perspective. *Global Biogeochemical Cycles* 32, 680–703. doi: 10.1002/2017GB005751

Hersbach, H., Bell, B., Berrisford, P., Hirahara, S., Horányi, A., Muñoz-Sabater, J., et al. (2020). The ERA5 global reanalysis. *Q. J. R. Meteorological Soc.* 146, 1999–2049. doi: 10.1002/qj.3803

Huang, T., Zhou, F., Ma, X., Zeng, D., Tang, Y., Ma, Y., et al. (2024). Characteristics and generation mechanisms of anticyclonic eddies, cyclonic eddies and dipole eddies in the Mozambique Channel. *Front. Mar. Sci.* 11, 1375367. doi: 10.3389/fmars.2024.1375367

Huggett, J., and Kyewalyanga, M. (2017). *The RV Dr Fridtjof Nansen in the Western Indian Ocean: Voyages of marine research and capacity development.* Eds. J. C. Groeneveld and K. A. Koranteng (Rome, Italy: FAO), 56–80.

José, Y. S., Aumont, O., Machu, E., Penven, P., Moloney, C. L., and Maury, O. (2014). Influence of mesoscale eddies on biological production in the Mozambique Channel: Several contrasted examples from a coupled ocean-biogeochemistry model. *Deep-sea Res. Part Ii-topical Stud. In Oceanography* 100, 79–93. doi: 10.1016/j.dsr2.2013.10.018

José, Y. S., Penven, P., Aumont, O., Machu, E., Moloney, C. L., Shillington, F., et al. (2016). Suppressing and enhancing effects of mesoscale dynamics on biological production in the Mozambique Channel. *J. Mar. Syst.* 158, 129–139. doi: 10.1016/j.jmarsys.2016.02.003

Koné, V., Aumont, O., Lévy, M., and Resplandy, L. (2009). "Physical and biogeochemical controls of the phytoplankton seasonal cycle in the Indian ocean: A modeling study," in *Indian Ocean Biogeochemical Processes and Ecological Variability.* Eds. J. D. Wiggert, R. R. Hood, S. W. A. Naqvi, K. H. Brink and S. L. Smith. Washington, D. C.: AGU, 147–166. doi: 10.1029/2008GM000700

Kyewalyanga, M., Naik, R., Hegde, S., Raman, M., Barlow, R., and Roberts, M. (2007). Phytoplankton biomass and primary production in Delagoa Bight, Mozambique: Application of remote sensing. *Estuarine Coast. Shelf Sci.* 74, 429–436. doi: 10.1016/j.ecss.2007.04.027

Lamont, T., Barlow, R. G., Morris, T., and van den Berg, M. A. (2014). Characterization of mesoscale features and phytoplankton variability in the Mozambique Channel. *Deep Sea Res. Part II: Topical Stud. Oceanography* 100, 94–105. doi: 10.1016/j.dsr2.2013.10.019

Lamont, T., Roberts, M., Barlow, R., Morris, T., and van den Berg, M. (2010). Circulation patterns in the Delagoa Bight, Mozambique, and the influence of deep ocean eddies. *Afr. J. Mar. Sci.* 32, 553–562. doi: 10.2989/1814232X.2010.538147

Landry, M. R., Brown, S. L., Rii, Y. M., Selph, K. E., Bidigare, R. R., Yang, E. J., et al. (2008). Depth-stratified phytoplankton dynamics in Cyclone Opal, a subtropical mesoscale eddy. *Deep Sea Res. Part II: Topical Stud. Oceanography* 55, 1348–1359. doi: 10.1016/j.dsr2.2008.02.001

Langa, A. A., and Calil, P. H. (2020). On the role of physical processes on the surface chlorophyll variability in the Northern Mozambique Channel. *Ocean Dynamics* 70, 95–114. doi: 10.1007/s10236-019-01311-0

Leal, M. C., Sá, C., Nordez, S., Brotas, V., and Paula, J. (2009). Distribution and vertical dynamics of planktonic communities at Sofala Bank, Mozambique, Estuarine. *Coast. Shelf Sci.* 84, 605–616. doi: 10.1016/j.ecss.2009.07.028

Lévy, M., Shankar, D., André, J.-M., Shenoi, S. S. C., Durand, F., and de Boyer Montégut, C. (2007). Basin-wide seasonal evolution of the Indian Ocean's phytoplankton blooms. *J. Geophys. Res.* 112, C12014. doi: 10.1029/2007JC004090

Lutjeharms, J. R. E. (2006). "The agulhas current retroflection," in *The Agulhas Current* (Springer, Berlin, Heidelberg). doi: 10.1007/3-540-37212-1_6

Lutjeharms, J., and Da Silva, A. (1988). The Delagoa bight eddy. *Deep Sea Res. Part A. Oceanographic Res. Papers* 35, 619–634. doi: 10.1016/0198-0149(88)90134-3

Machu, E., Lutjeharms, J. R. E., Webb, A. M., and Van Aken, H. M. (2002). First hydrographic evidence of the southeast Madagascar upwelling cell. *Geophys. Res. Lett.* 29 (21), 2009. doi: 10.1029/2002GL015381

Malauene, B. S., Moloney, C. L., Lett, C., Roberts, M. J., Marsac, F., and Penven, P. (2018). Impact of offshore eddies on shelf circulation and river plumes of the Sofala Bank, Mozambique Channel. *J. Mar. Syst.* 185, 1–12. doi: 10.1016/j.jmarsys.2018.05.001

Malauene, B. S., Shillington, F. A., Roberts, M. J., and Moloney, C. L. (2014). Cool, elevated chlorophyll-a waters off northern Mozambique. *Deep-Sea Res. II Top. Stud. Oceanogr.* 100, (0) (68–8). Available at: http://www.sciencedirect.com/science/article/pii/S0967064513004116. (the Mozambique Channel: Mesoscale Dynamics and Ecosystem Responses).

Marsac, F., Barlow, R., Ternon, J. F., Ménard, F., and Roberts, M. (2014). Ecosystem functioning in the mozambique channel: Synthesis and future research. *Deep Sea Res. Part II: Topical Stud. Oceanography* 100, 212–220. doi: 10.1016/j.dsr2.2013.10.028

Mason, E., Pascual, A., Gaube, P., Ruiz, S., Pelegrí, J. L., and Delepoulle, A. (2017). Subregional characterization of mesoscale eddies across the Brazil-Malvinas Confluence. *J. Geophys. Res. Oceans* 122, 3329–3357. doi: 10.1002/2016JC012611

Mason, E., Pascual, A., and McWilliams, J. C. (2014). A new sea surface height–based code for oceanic Mesoscale Eddy tracking. *J. Atmos. Oceanic Technol.* 31, 1181–1188. doi: 10.1175/JTECH-D-14-00019.1

Mason, E., Ruiz, S., Bourdalle-Badie, R., Reffray, G., García-Sotillo, M., and Pascual, A. (2019). New insight into 3-D mesoscale eddy properties from CMEMS operational models in the western Mediterranean. *Ocean Sci.* 15, 1111–1131. doi: 10.5194/os-15-1111-2019

McGillicuddy, D. J. (2016). Mechanisms of physical-biological-biogeochemical interaction at the oceanic mesoscale. *Mar. Sci.* 8, 125–159. doi: 10.1146/annurev-marine-010814-015606

McGillicuddy, D. J., Anderson, L. A., Bates, N. R., Bibby, T., Buesseler, K. O., Carlson, C. A., et al. (2007). Eddy/wind interactions stimulate extraordinary mid-ocean plankton blooms. *Science* 316, 1021–1026. doi: 10.1126/science.1136256

McGillicuddy, D. J., Anderson, L. A., Doney, S. C., and Maltrud, M. E. (2003). Eddy-driven sources and sinks of nutrients in the upper ocean: Results from a 0.1° resolution model of the North Atlantic. *Global Biogeochemical Cycles* 17, 1035. doi: 10.1029/2002GB001987

Moore, T. S. II, Matear, R. J., Marra, J., and Clementson, L. (2007). Phytoplankton variability off the Western Australian Coast: Mesoscale eddies and their role in cross-shelf exchange. *Deep Sea Res. Part II: Topical Stud. Oceanography* 54, 943–960. doi: 10.1016/j.dsr2.2007.02.006

Morrow, R., Birol, F., Griffin, D., and Sudre, J. (2004). Divergent pathways of cyclonic and Anticyclonic eddies. *Geophys. Res. Lett.* 31, L24311. doi: 10.1029/2004GL020974

Ning, J., Chen, K., and Gaube, P. (2021). Diverse variability of surface chlorophyll during the evolution of Gulf Stream rings. *Geophysical Res. Lett.* 48, e2020GL091461. doi: 10.1029/2020GL091461

Omta, A. W., Llido, J., Garçon, V., Kooijman, S. A. L. M., and Dijkstra, H. A. (2009). The interpretation of satellite chlorophyll concentrations: the case of the Mozambique Channel. *Deep-Sea Res. I* 56, 974–988. doi: 10.1016/j.dsr.2009.01.011

Paula, J., Pinto, I., Guambe, I., Monteiro, S., and Gove, D. (1998). Seasonal cycle of planktonic communities at Inhaca Island, southern Mozambique. *J. Plankton Res.* 20, 2165–2178. doi: 10.1093/plankt/20.11.2165

Penven, P., Echevin, V., Pasapera, J., Colas, F., and Tam, J. (2005). Average circulation, seasonal cycle, and mesoscale dynamics of the Peru Current System: A modeling approach. *J. Geophys. Res.* 110, C10021. doi: 10.1029/2005JC002945

Pereira, F., da Silveira, I. C. A., Tandon, A., Franks, P. J. S., Luko, C. D., Santos, D. M. C., et al. (2024). Phytoplankton responses to mesoscale and submesoscale processes in a tropical meander. *J. Geophysical Research: Oceans* 129, e2023JC020685. doi: 10.1029/2023JC020685

Quartly, G. D., Buck, J. J. H., Srokosz, M. A., and Coward, A. C. (2006). Eddies around Madagascar – The Retroflection re-considered. *J. Mar. Sys.* 63, 115–129. doi: 10.1016/j.jmarsys.2006.06.001

Quartly, G. D., de Cuevas, B. A., and Coward, A. C. (2013). Mozambique Channel eddies in GCMs: A question of resolution and slippage. *Ocean Model.* 63, 56–67. doi: 10.1016/j.ocemod.2012.12.011

Renault, L., McWilliams, J. C., and Penven, P. (2017). Modulation of the Agulhas Current Retroflection and Leakage by oceanic current interaction with the atmosphere. *J. Phys. Oceanogr.* 47, 2077–2100. doi: 10.1175/JPO-D-16-0168.1

Roberts, M. J., Ternon, J.-F., and Morris, T. (2014). Interaction of dipole eddies with the western continental slope of the Mozambique Channel. *Deep Sea Res. Part II: Topical Stud. Oceanography* 100, 54–67. doi: 10.1016/j.dsr2.2013.10.016

Rodriguez, F., Varela, M., Fernández, E., and Zapata, M. (2003). Phytoplankton and pigment distributions in an anticyclonic slope water oceanic eddy (SWODDY) in the southern Bay of Biscay. *Mar. Biol.* 143, 995–1011. doi: 10.1007/s00227-003-1129-1

Sá, C., Leal, M., Silva, A., Nordez, S., André, E., Paula, J., et al. (2013). Variation of phytoplankton assemblage salong the Mozambique coast as revealed by HPLC and microscopy. *J. Sea Res.* 79, 1–11. doi: 10.1016/j.seares.2013.01.001

Sætre, R., and Paula Da Silva, R. (1979). *The marine fish resources of Mozambique* (Bergen, Norway: Institute of Marine Research).

Schouten, M. W., de Ruijter, W. P., Van Leeuwen, P. J., and Ridderinkhof, H. (2003). Eddies and variability in the mozambique channel. *Deep Sea Res. Part II: Topical Stud. Oceanography* 50 (12-13), 1987–2003. doi: 10.1016/S0967-0645(03)00042-0

Schulien, J. A., Della Penna, A., Gaube, P., Chase, A. P., Haëntjens, N., Graff, J. R., et al. (2020). Shifts in phytoplankton community structure across an anticyclonic eddy revealed from high spectral resolution lidar scattering measurements. *Front. Mar. Sci.* 7. doi: 10.3389/fmars.2020.00493

Shchepetkin, A., and McWilliams, J. C. (2005). The Regional Oceanic Modeling System: A split-explicit, free-surface, topography-following-coordinate ocean model. *Ocean Model.* 9, 347–404. doi: 10.1016/j.ocemod.2004.08.002

Smith, G. C., and Fortin, A.-S. (2022). Verification of eddy properties in operational oceanographic analysis systems. *Ocean Modell.* 172, 101982. doi: 10.1016/j.ocemod.2022.101982

Swart, N. C., Lutjeharms, J. R. E., Ridderinkhof, H., and de Ruijter, W. P. M. (2010). Observed characteristics of Mozambique Channel eddies. *J. Geophys. Res.* 115, C09006. doi: 10.1029/2009JC005875

Tew-Kai, E., and Marsac, F. (2009). Patterns of variability of sea surface chlorophyll in the Mozambique Channel: a quantitative approach. *J. Mar. Syst.* 77, 77–88. doi: 10.1016/j.jmarsys.2008.11.007. ISSN 0924-7963.

Waite, A. M., Pesant, S., Griffin, D. A., Thompson, P. A., and Holl, C. M. (2007). Oceanography, primary production and dissolved inorganic nitrogen uptake in two Leeuwin Current eddies. *Deep Sea Res. Part II: Topical Stud. Oceanography* 54, 981–1002. doi: 10.1016/j.dsr2.2007.03.001

Weimerskirch, H., Le Corre, M., Jaquemet, S., Potier, M., and Marsac, F. (2004). Foraging strategy of a top predator in tropical waters: great frigatebirds in the mozambique channel. *Mar. Ecol. Prog. Ser.* 275, 297–308. doi: 10.3354/meps275297

Williams, R. G., and Follows, M. J. (1998). The Ekman transfer of nutrients and maintenance of new production over the North Atlantic. *Deep-Sea Res. I* 45, 461–489. doi: 10.1016/S0967-0637(97)00094-0. I: Topical Studies in Oceanography, 54(8-10), 943-960.